0013-7227/02/$15.00/0
Printed in U.S.A.

Endocrinology 143(7):2797–2807

Prevention of Thecal Angiogenesis, Antral Follicular Growth, and Ovulation in the Primate by Treatment with Vascular Endothelial Growth Factor Trap R1R2

CHRISTINE WULFF, HELEN WILSON, STANLEY J. WIEGAND, JOHN S. RUDGE, AND HAMISH M. FRASER

Medical Research Council (C.W., H.W., H.M.F.) Human Reproductive Sciences Unit, Edinburgh, United Kingdom EH3 9ET; Department of Obstetrics and Gynecology, University of Ulm (C.W.), 89075 Ulm, Germany; and Regeneron Pharmaceuticals, Inc. (S.J.W., J.S.R.), Tarrytown, New York 10591

This study was designed to investigate the effects of inhibition of thecal angiogenesis on follicular development in the marmoset monkey (*Callithrix jacchus*). To inhibit vascular endothelial growth factor (VEGF), a soluble combined truncated form of the fms-like tyrosine kinase (Flt) and kinase insert domain-containing receptor (KDR) receptor fused to IgG (VEGF Trap R1R2) was administered for 10 d during the follicular phase of the cycle. Changes in angiogenesis and follicular cell proliferation were quantified using immunocytochemistry for bromodeoxyuridine to obtain a proliferation index, CD31 to visualize endothelial cell area, and dual staining to distinguish thecal endothelial cell proliferation. The effects of the treatment on follicular development were assessed by morphometric analyses by measuring follicle diameter, thecal thickness, and a proliferation index for granulosa cells. Follicular atresia was detected and quantified using the terminal deoxynucleotidyltransferase-UTP nick end labeling method. Effects on gene expression of VEGF and its receptors, Flt and KDR, were studied by *in situ* hybridization. VEGF Trap R1R2 treatment resulted in a significant decrease in thecal proliferation and endothelial cell area, demonstrating the suppression of thecal angiogenesis. The absence of a normal thecal vasculature was associated with a significantly reduced thecal thickness. Antral follicular development was severely compromised, as indicated by decreased granulosa cell proliferation, decreased follicular diameter, and lack of development of ovulatory follicles. Furthermore, the rate of atresia was significantly increased. VEGF expression in granulosa and thecal cells increased after treatment, whereas Flt and KDR expressions in thecal endothelial cells were markedly decreased. These results show that VEGF Trap treatment is associated with the suppression of follicular angiogenesis, which results in the inhibition of antral follicular development and ovulation. (*Endocrinology* 143: 2797–2807, 2002)

THE OVARY IS distinctive in being a site of active angiogenesis in the adult. Angiogenesis takes place in the developing follicle before ovulation and in the corpus luteum formed postovulation (1–4). It is now well established that active cyclical angiogenesis plays a key role in normal luteal function (1, 4). However, its contribution to normal follicular growth and function has not been addressed experimentally. Thus, little is known about the direct relevance of the thecal vasculature for follicular growth, development, and atresia. Although small preantral follicles are avascular, angiogenesis is initiated during early follicular development and continues throughout follicular growth. The vascular sheath that develops during follicular maturation in the thecal compartment expands with ongoing folliculogenesis (3). The thecal capillaries do not penetrate the membrana propria, so the granulosa compartment remains avascular until breakdown of the basement membrane at ovulation.

The vasculature of the follicle is thought to be necessary for the delivery of hormones, hormone precursors, oxygen, and nutrients. It has been suggested that the preferential delivery of gonadotropins via a more highly developed vascular system in individual follicles plays an instrumental role in the selection and growth of the dominant follicle (5). The relationship between changes in angiogenesis and onset of atresia is uncertain due to difficulties in determining the temporal relationship between these processes, but decreased vascularity in atretic follicles has been reported in a number of species (5–7), including the marmoset (3).

With regard to the molecular mechanisms controlling follicular angiogenesis, the presence of the vascular endothelial growth factor (VEGF), a principal angiogenic factor, has been described in the ovarian follicle (8, 9). More recently, we have demonstrated by direct inhibition of VEGF *in vivo* in the primate that VEGF is a major regulator of follicular angiogenesis (3). Inhibition of VEGF was followed by a severe restriction of thecal angiogenesis in the developing follicle. To investigate the importance of the thecal vasculature for follicular maturation, the approach of suppressing thecal angiogenesis by *in vivo* inhibition of VEGF was used in the current study. A new compound, VEGF Trap R1R2, comprising the extracellular domain of the two VEGF receptors, VEGF-R1 (Flt) (fms-like tyrosine kinase) and VEGF-R2 (KDR) (kinase insert domain-containing receptor), was administered to marmoset monkeys throughout the follicular phase. The efficacy of VEGF Trap R1R2 to suppress thecal angiogenesis was tested using bromodeoxyuridine (BrdU) immunocytochemistry as a proliferation marker, CD31 as a specific endothelial cell marker and dual staining to dis-

Abbreviations: BrdU, Bromodeoxyuridine; Flt, fms-like tyrosine kinase; KDR, kinase insert domain-containing receptor; NBT, nitro blue tetrazolium; TBS, Tris-buffered saline; TUNEL, terminal deoxynucleotidyltransferase-UTP nick end labeling; VEGF, vascular endothelial growth factor.

tinguish between proliferating endothelial and nonendothelial cells. The influence on follicular development was assessed by morphological and morphometric image analyses as well as quantification of granulosa cell proliferation. As granulosa cells of the follicle die of apoptosis during the process of atresia (10), the terminal deoxynucleotidyltransferase-UTP nick end labeling (TUNEL) method was used to detect apoptotic granulosa cells for definite classification and quantification of atretic follicles. The effects of inhibition of VEGF on the expression of VEGF and its receptors Flt and KDR was investigated using *in situ* hybridization.

Materials and Methods

VEGF Trap R1R2

The VEGF Trap R1R2 used in these experiments is a recombinant chimeric protein comprising portions of the extracellular, ligand binding domains of the human VEGF receptors Flt-1 (VEGF-R1, Ig domain 2) and KDR (VEGF-R2, Ig domain 3) expressed in sequence with the Fc portion of human IgG (Fig. 1). The presence of the Fc domain results in homodimerization of the recombinant protein, thereby creating a high affinity (KD1–5pM) VEGF Trap.[1] The VEGF trap was expressed in CHO cells and was purified by protein A affinity chromatography followed by size-exclusion chromatography. The specificity of VEGF binding and the affinity to VEGF of VEGF Trap R1R2 were determined by Biacore (Uppsala, Sweden).

Animals

Adult female common marmoset monkeys (*Callithrix jacchus*) with a body weight of approximately 350 g and regular ovulatory cycles (28-d cycle length) with ovulation on d 8 were housed together with a younger sister or prepubertal female as described previously (11). Blood samples were collected three times per week by femoral venipuncture without anesthesia, and plasma was subjected to progesterone assay as described previously (4).

Treatment

Experiments were carried out in accordance with the Animals (Scientific Procedures) Act, 1986, and were approved by the local ethical review process committee. To synchronize timing of ovulation during the pretreatment cycle, marmosets were given $PGF_{2\alpha}$ in the mid to late luteal phase to induce luteolysis. In the late luteal phase of the subsequent cycle, four marmosets were treated with VEGF trap at a dose of 25 mg/kg, injected sc on d 0, 2, 4, 6, and 8 of the follicular phase. Ovaries were collected 2 d later on d 10 of the cycle. Eleven control marmosets were studied (four on d 1–2, three on d 7–8, and four at d 11 of the cycle). Control animals were treated with vehicle containing 5 mM phosphate, 5 mM citrate, 100 mM sodium chloride, 0.1% (wt/vol) Tween 20, and 20% (wt/vol) sucrose. All animals were injected iv with 20 mg BrdU (Roche Molecular Biochemicals, Essex, UK) in saline 1 h before being sedated using 100 μl ketamine hydrochloride (Parke-Davis Veterinary, Pontypool, UK) and killed with an iv injection of 400 μl Euthetal (sodium pentobarbitone, Rhone Merieux, Harlow, UK). After cardiac exsanguination via a heparinized syringe, ovaries were removed immediately and fixed in 4% neutral buffered formalin. After 24 h, the ovaries were put into 70% ethanol, dehydrated, and embedded in paraffin according to standard procedures.

Hematoxylin-eosin staining

The embedded ovaries were serially sectioned, and tissue sections (5 μm) were placed onto BDH SuperFrost slides (BDH, Merck & Co., Inc., Poole, UK). For morphological and morphometric analyses every 20 of a total of 200 sections/ovary were used. Sections in between were subjected to immunocytochemistry, *in situ* hybridization, and TUNEL. Tissue sections were dewaxed in xylene, rehydrated in descending concentrations of ethanol, washed in distilled water, and stained with hematoxylin (Richard-Allan, Richland, MI) for 5 min, followed by a wash in water and acetic alcohol before staining with eosin (Richard-Allan) for 20 sec. After dehydrating in ascending concentrations of ethanol and xylene, sections were mounted.

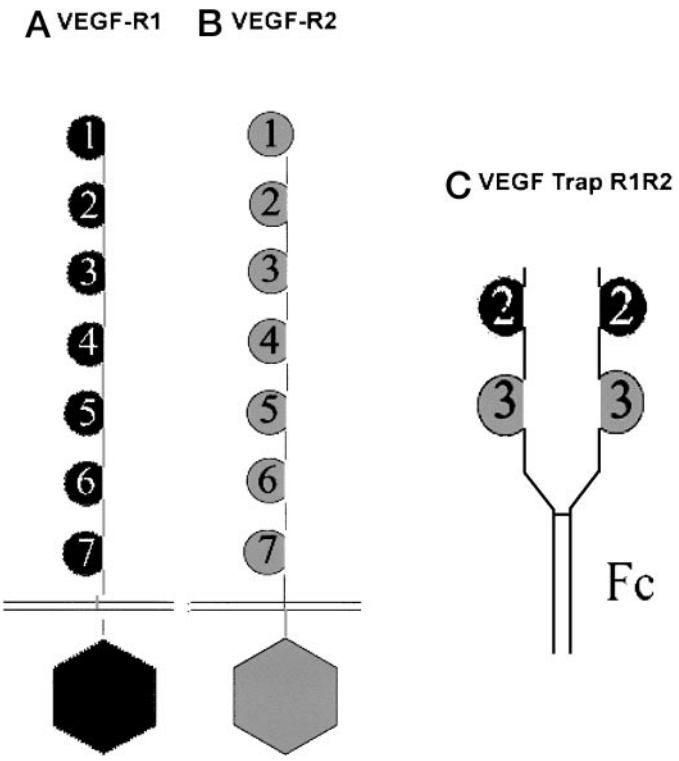

FIG. 1. Structure of VEGF receptors and the VEGF Trap. VEGF-R1 (A) and VEGF-R2 (B) both contain seven extracellular domains, which differ between the two receptors. These extracellular domains are responsible for VEGF binding. The soluble VEGF Trap R1R2 (C) was created by fusion of domain 2 of VEGF-R1 and domain 3 of VEGF-R2 with the FC portion of IgG.

Immunocytochemistry

The effects of the treatment on the establishment of the thecal vascular network were studied by 1) quantifying the number of proliferating cells stained for BrdU, 2) identifying endothelial cells using CD31 staining, and 3) distinguishing proliferating endothelial from nonendothelial cells by colocalization of BrdU and CD31.

For BrdU and CD31 immunostaining, antigen retrieval was performed by pressure cooking (Tefal Clypso pressure cooker, Tefal, Essex, UK) sections in 0.01 M citrate buffer, pH 6, for 6 min at high pressure setting 2. Slides were then left for 20 min in hot buffer and washed in TBS (0.05 mol/liter Tris and 9 g/liter NaCl). To reduce nonspecific binding sections were blocked in normal rabbit serum (1:5 diluted in TBS containing 5% BSA) for 30 min. Primary antibodies CD31 (mouse antihuman CD31, DAKO Corp., Copenhagen, Denmark) or BrdU (mouse anti-BrdU, Roche Molecular Biochemicals) were diluted 1:20 or 1:30 in TBS, respectively. Incubation was carried out overnight at 4 C. Slides were washed three times in TBS. Incubation with the secondary antibody, rabbit antimouse Ig (1:60 diluted in NRS:TBS; DAKO Corp.), was performed for 40 min at room temperature, followed after two washes in TBS by incubation of the alcaline phosphatase-antialcaline phospholase (APAAP) complex (1:100 dilution in TBS, DAKO Corp.) for 40 min at room temperature. Visualization was performed using 500 μl/slide nitro blue tetrazolium (NBT) solution containing 45 μl NBT substrate (Roche Molecular Biochemicals), 10 ml NBT buffer, 35 μl 5-bromo-3-chloro-3-indolyl-phosphate, and 10 μl levamisole. Sections for BrdU

[1] The detailed molecular structure and how it was created are described in the patent REG 710-A-PCT, VEGF Trap Application published December 2000, Publication WO 00/75319 A1.

were counterstained with hematoxylin, whereas sections for CD31 were not counterstained, so that quantitative image analysis could be performed. For dual labeling, slides were incubated first with CD31 and visualization with Fast Red [Sigma, Poole, UK; 1 mg Fast Red in 1 ml Fast Red buffer (20 mg naphtol AS-MX phosphate, 2 ml dimethyl formamide, and 98 ml 0.1 M Tris, pH 8.2)]. After staining for CD31, incubation with BrdU was performed. BrdU-stained cells were visualized with NBT as described above.

In situ hybridization

In situ hybridization was performed as described previously (4, 12). As the marmoset shows 97–98% homology of the known gene sequence with human genome, cRNA probes for human VEGF, Flt, and KDR were used. Sense and antisense probes were prepared using an RNA transcription kit (Ambion, Inc. Austin, TX) and were labeled with [^{35}S]-uridine 5[prime]-triphosphate (NEN Life Science Products, Boston, MA). Deparaffinized sections were treated with 0.1 N HCl and then digested in proteinase K (5 μg/ml; Sigma) for 30 min at 37 C. After prehybridization for 2 h at 55 C subsequent hybridization was performed in a moist chamber overnight. High stringency posthybridization washings and ribonuclease treatment were used to remove excess probe. Slides were then dehydrated, dried, and dipped in Ilford G5 liquid emulsion (H. A. West, Edinburgh, UK). Exposure times for VEGF, Flt, and KDR were 4, 7, and 7 wk, respectively. Slides were subsequently developed (D19 developer, Kodak, Rochester, NY) and fixed (GBS, Kodak). All slides were counterstained with hematoxylin (Richard-Allan, Richland, MI), dehydrated, and mounted.

In situ TUNEL

It is known that during atresia granulosa cells undergo programmed cell death, apoptosis. Hence, the TUNEL method for detection of apoptotic cells was used to identify atretic follicles. Dewaxed and rehydrated slides were incubated for 6 min in 20 μg/ml proteinase K (Sigma) at room temperature and blocked with normal sheep serum (1:5 dilution). Slides were washed three times in TBS. For 3′-end labeling the TdT Kit (Roche Molecular Biochemicals) was used. 3′-OH ends of DNA fragments were labeled with 1 nM digoxigenin-11-deoxy-UTP (Roche Molecular Biochemicals) for 1.5 h at 37 C by 1 IU/μl TdT (Roche Molecular Biochemicals) in 50 μl buffer [30 mM Tris-HCl (pH 7.2), 140 mM sodium cacodylate, and 1.5 mM $CoCl_2$; Roche Molecular Biochemicals). Negative control slides had the TdT replaced by the equivalent amount of buffer. Three rinses of the slides with TBS were followed by incubation with alkaline phosphatase-conjugated sheep anti-digoxigenin antibodies (1:100 dilution; Roche Molecular Biochemicals) in TBS for 90 min at room temperature. The labeling was visualized with NBT as described above. After air-drying, slides were put into xylene and mounted.

Analysis of data

Quantitative analysis was performed using an image analysis system linked to an Olympus Corp. camera, and the data were processed using Image-Pro Plus version 3.0 for Windows (Microsoft Corp.).

Morphological characterization of ovarian follicles

Stages of follicular development were defined as follows: primary follicles (containing only one granulosa cell layer), early secondary follicles (two to four granulosa cell layers, no antrum), late secondary follicles (more than four granulosa cell layers, no antrum), tertiary follicles (follicles containing an antrum), and ovulatory follicles (large antral follicles, >2 mm). Follicles were classified as healthy if they contained a normal-shaped oocyte surrounded by granulosa cells that were regularly apposed on an intact basement membrane with normal appearance of granulosa cell nuclei without signs of pycnosis. Follicles not fulfilling these criteria were classified as unsuitable for analyses. Only follicles with a visible oocyte containing a nucleus were considered to ensure proper follicular classification.

Morphometric analyses

Serial sections of both ovaries of each animal stained for hematoxylin-eosin were subjected to morphometric analyses (10 sections at a distance of 100 μm/ovary from each other). A total of 31 primary, 523 secondary, and 181 tertiary follicles were analyzed in controls, and 29 primary, 327 secondary, and 77 tertiary follicles were analyzed in treated animals. The image analysis system was set up to measure two diameters of the follicles in a right angle. From these diameters the mean follicular diameter was calculated. Furthermore, the thecal compartment was outlined, and the mean thecal thickness was measured.

Quantification of immunocytochemistry, in situ hybridization, and 3′-end labeling

From our previous study (3) it was known that angiogenesis is initiated in follicles containing more than four granulosa cell layers. Thus, in this study only follicles with four or more granulosa cell layers were analyzed. In all follicles the whole cross-sections were analyzed. Captured images were thresholded, and the thecal and granulosa cell compartments were outlined and analyzed separately.

BrdU labeling

Four sections per ovary were analyzed under ×200 magnification. The image analysis system was set up to measure the number of dark-stained nuclei (BrdU positive), and the number of dark- and light-stained nuclei (total number of cells) in the outlined compartment of interest. A proliferation index (*i.e.* BrdU-positive cells expressed as a percentage of the total number of cells) was calculated in the thecal and granulosa compartments for each follicle. The proliferation index was expressed as a mean value for the number of follicles assessed within each follicular stage and per animal.

The automated image analysis of BrdU in the granulosa of secondary follicles failed to reliably distinguish between single cells because granulosa cells have only a small cytoplasmic volume, so that the nuclei of different cells are in close vicinity. Thus, the granulosa cell proliferation index in these follicles was obtained by manual counting using an eyepiece with a grid.

CD31 labeling

The endothelial cell area (*i.e.* CD31-positive cells) was measured at ×200 magnification in four sections of each ovary. The captured gray scale image was thresholded and converted to a binary image. The whole area of the thecal compartment and the CD31-positive area within the compartment was measured. The CD31-positive area was then calculated per unit area of the thecal compartment and expressed as a mean value for the number of follicles assessed within each follicular stage and per animal.

3′-End labeling

Four sections per animal were analyzed. Follicles were classified as atretic if more than approximately 20% of the granulosa cells were apoptotic. The number of atretic and healthy late secondary and antral follicles were counted manually, and an index for atresia (atretic follicles expressed as a percentage of total number of follicles) was calculated.

Statistical analysis

Data obtained for different cycle and follicular stages were tested for significant differences using ANOVA, followed by Duncan's multiple range test. Effects of the treatment compared with late follicular controls were determined using a two-tailed, unpaired *t* test. Differences were considered to be significant at $P < 0.05$. The tests were performed using SPSS version 6.1 for Macintosh (SPSS, Inc., Chicago, IL). All values are given as the mean ± SEM.

Results

Efficacy of the treatment to suppress thecal angiogenesis

Dual staining for BrdU and CD31 (Fig. 2A) showed the established microvasulature in controls. Besides numerous single-stained cells for BrdU, some BrdU-positive cells were also associated with CD31 staining, indicating proliferating

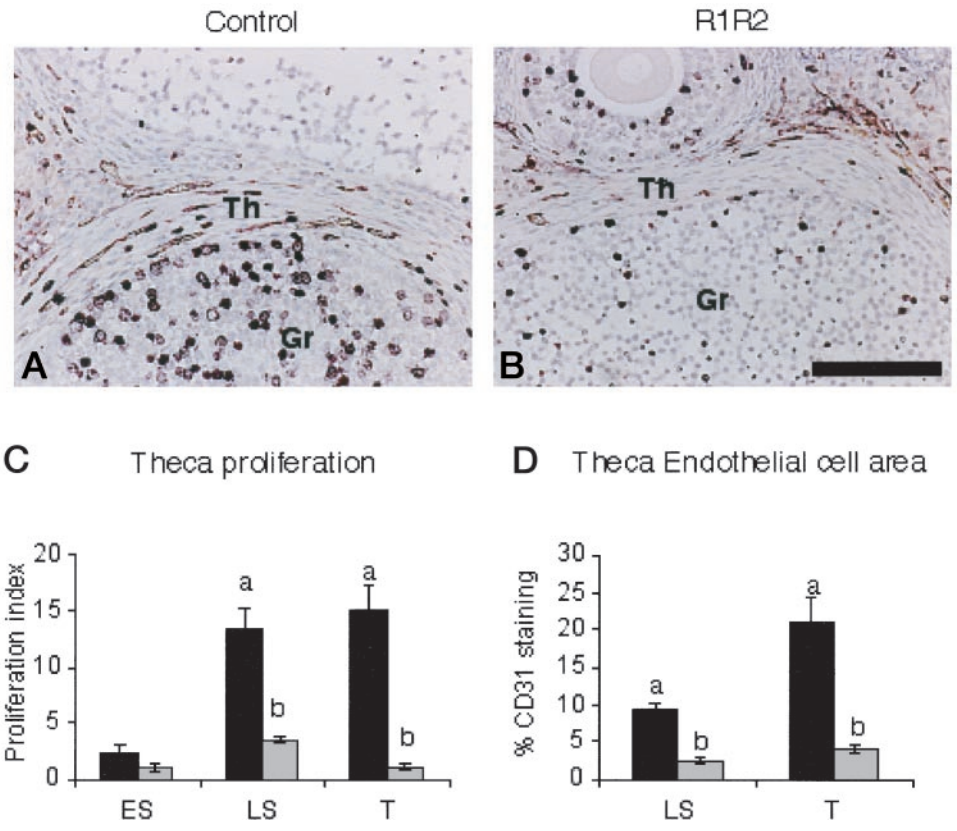

FIG. 2. Dual staining for CD31 (*red* staining) and BrdU (*black* nuclei) in a follicle of a control (A) and an R1R2-treated animal (B). Note the reduction of proliferating cells (single and dual stained) and endothelial staining in the theca (Th) after treatment. Quantification of thecal proliferation (C) revealed a significant decrease in late secondary (LS) and tertiary (T) follicles. In these follicle stages the endothelial cell area (D) was also significantly reduced, demonstrating the suppression of thecal angiogenesis after treatment. Different letters indicate significant differences. ■, controls; ▨, R1R2 treated. ES, Early secondary follicle. *Bar*, 100 μm.

endothelial cells. After R1R2 treatment (Fig. 2B), very few proliferating cells were visible, and thecal CD31 staining was markedly reduced. These observations were confirmed by quantitative analyses (Fig. 2, C and D). The thecal proliferation index in late secondary follicles was 13.6 ± 2.8% in early follicular controls, 13.2 ± 1.8% in late follicular controls, and 13.4 ± 1.4% in early luteal controls. After treatment, a 79% reduction ($P < 0.05$) of thecal proliferation was found in late secondary follicles (3.4 ± 0.6%). The thecal proliferation index of tertiary follicles was 10.6 ± 0.4% in early follicular controls, 15.1 ± 2.1% in late follicular controls, and 16.2 ± 2.0% in early luteal controls. After R1R2 treatment, a major 92% reduction ($P < 0.001$) in thecal proliferation in tertiary follicles (1.1 ± 0.2%) was observed.

The endothelial cell areas measured in secondary or tertiary follicles of control animals were comparable (in secondary follicles, 0.09 ± 0.01 μm^2/unit area during the early follicular phase, 0.09 ± 0.008 μm^2/unit area during the late follicular phase, and 0.09 ± 0.008 μm^2/unit area during the early luteal phase; in tertiary follicles, 0.2 ± 0.01 μm^2/unit area during the early follicular phase, 0.2 ± 0.03 μm^2/unit area during the late follicular phase, and 0.18 ± 0.02 μm^2/unit area during the early luteal phase). After R1R2 treatment a significant reduction of the endothelial cell area of 72% was found in secondary follicles (0.025 ± 0.005 μm^2/unit area) and 80% in tertiary follicles (0.04 ± 0.007 μm^2/unit area). In summary, it was evident that the treatment efficiently suppressed thecal angiogenesis in secondary and tertiary follicles.

Effects of R1R2 treatment on thecal development

Thecal development is initiated during early follicular growth when a follicle contains more than two granulosa cell layers. The fully differentiated theca is shown in Fig. 3A. Thecal cells have an elongated flat appearance surrounding the granulosa compartment in several layers. Fibrocytes are dispersed within these layers as the microvasculature is established. After R1R2 treatment (Fig. 3B), thecal cells appeared swollen, contained enlarged nuclei, and had lost their elongate shape. Furthermore, the theca lacks a microvasculature. In contrast, the occurrence of fibrocytes appeared unaffected.

By measuring thecal thickness and plotting against the follicular diameter (Fig. 3C), a significant linear correlation was found for secondary follicles in controls ($r = 0.9$; $P < 0.001$) and treated animals ($r = 0.86$; $P < 0.001$). However, after R1R2 treatment the slope of the curve was reduced, indicating that at a given follicle diameter the theca is thinner than that in controls. Comparison of the mean thecal thickness in these follicles confirmed a significant reduction ($P < 0.05$) in thecal thickness after treatment. No correlation between thecal thickness and follicle diameter was observed in tertiary follicles.

Effects of R1R2 treatment on the expression of VEGF and its receptors KDR and Flt

In controls, VEGF mRNA was expressed in the granulosa and to a lesser extent in the thecal compartment in secondary and tertiary follicles (Fig. 4A). An increase in

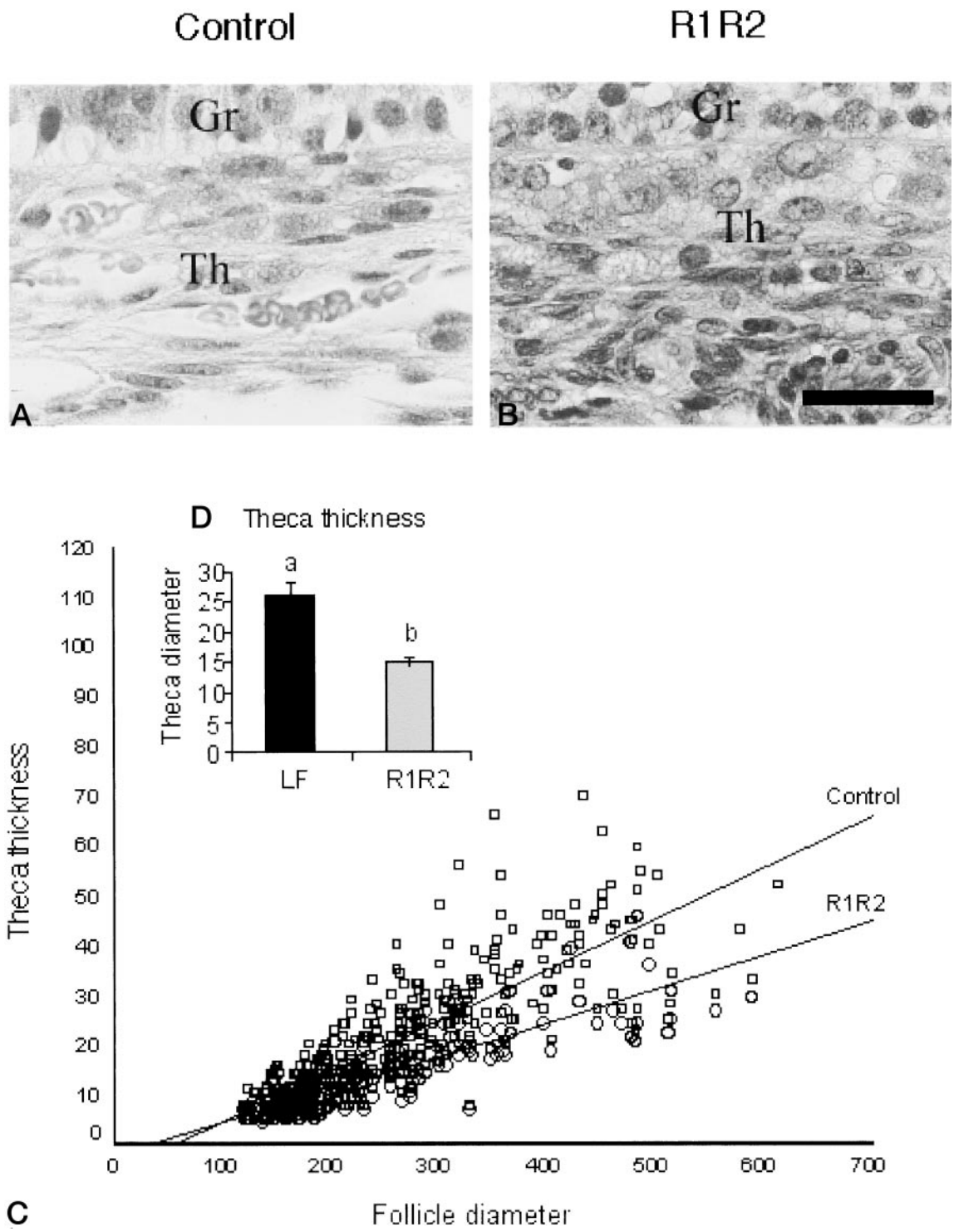

FIG. 3. Effects of the inhibition of thecal angiogenesis on thecal development. A, A hematoxylin- and eosin-stained section of the theca (Th) of a control. Thecal cells have an elongated, flattened shape. Capillaries pass through the thecal compartment. B, Thecal cells after R1R2 treatment appear swollen with enlarged nuclei. Note the lack of the thecal capillaries (*bar*, 100 μm). Measuring the thecal thickness and plotting it against the follicle diameter (C), a significant linear correlation for both in controls and after R1R2 treatment was found. However, the curve for the R1R2 treatment exhibited a lower slope, indicating that the theca after treatment is thinner. This was confirmed by comparison of the mean thecal diameters (D). *Different letters* indicate significant differences. LF, Late follicular control.

DOCKET ALARM

Explore Litigation Insights

Docket Alarm provides insights to develop a more informed litigation strategy and the peace of mind of knowing you're on top of things.

Real-Time Litigation Alerts

Keep your litigation team up-to-date with **real-time alerts** and advanced team management tools built for the enterprise, all while greatly reducing PACER spend.

Our comprehensive service means we can handle Federal, State, and Administrative courts across the country.

Advanced Docket Research

With over 230 million records, Docket Alarm's cloud-native docket research platform finds what other services can't. Coverage includes Federal, State, plus PTAB, TTAB, ITC and NLRB decisions, all in one place.

Identify arguments that have been successful in the past with full text, pinpoint searching. Link to case law cited within any court document via Fastcase.

Analytics At Your Fingertips

Learn what happened the last time a particular judge, opposing counsel or company faced cases similar to yours.

Advanced out-of-the-box PTAB and TTAB analytics are always at your fingertips.

API

Docket Alarm offers a powerful API (application programming interface) to developers that want to integrate case filings into their apps.

LAW FIRMS
Build custom dashboards for your attorneys and clients with live data direct from the court.

Automate many repetitive legal tasks like conflict checks, document management, and marketing.

FINANCIAL INSTITUTIONS
Litigation and bankruptcy checks for companies and debtors.

E-DISCOVERY AND LEGAL VENDORS
Sync your system to PACER to automate legal marketing.